

Many-body perturbation theory of frequency-dependent polarizabilities and van der Waals coefficients: Application to H₂O–H₂O and Ar–NH₃

Cite as: J. Chem. Phys. **97**, 5592 (1992); <https://doi.org/10.1063/1.463767>

Submitted: 17 January 1992 . Accepted: 07 July 1992 . Published Online: 31 August 1998

Paul E. S. Wormer, and Hinne Hettema



View Online



Export Citation

ARTICLES YOU MAY BE INTERESTED IN

[Correlated van der Waals coefficients. II. Dimers consisting of CO, HF, H₂O, and NH₃](#)

The Journal of Chemical Physics **90**, 6507 (1989); <https://doi.org/10.1063/1.456317>

[Levels of symmetry adapted perturbation theory \(SAPT\). I. Efficiency and performance for interaction energies](#)

The Journal of Chemical Physics **140**, 094106 (2014); <https://doi.org/10.1063/1.4867135>

[An improved simple model for the van der Waals potential based on universal damping functions for the dispersion coefficients](#)

The Journal of Chemical Physics **80**, 3726 (1984); <https://doi.org/10.1063/1.447150>

Lock-in Amplifiers

Zurich Instruments

Watch the Video

Many-body perturbation theory of frequency-dependent polarizabilities and van der Waals coefficients: Application to H₂O–H₂O and Ar–NH₃

Paul E. S. Wormer and Hinne Hettema

Institute of Theoretical Chemistry, University of Nijmegen, Toernooiveld, 6525 ED Nijmegen, The Netherlands

(Received 17 January 1992; accepted 7 July 1992)

Correlation contributions to the multipole moments and frequency dependent polarizabilities of molecules are described within the framework of time-dependent coupled Hartree–Fock and many-body perturbation theory. Computationally feasible expressions are given for the “true” correlation contributions to the multipole moments and frequency dependent polarizabilities. The polarizabilities of argon, ammonia and water and the van der Waals induction and dispersion coefficients of H₂O–H₂O and Ar–NH₃ are presented.

I. INTRODUCTION

With the advent of far-infrared laser spectroscopy of van der Waals molecules in molecular beams^{1–3} a tool has become available that probes very sensitively intermolecular potential energy surfaces.⁴ In principle, one can obtain an energy surface from a rovibrational spectrum by first guessing a parametrized surface and then solving the rovibrational problem. Comparison of the solution with experiment will then suggest an improved set of energy parameters and, by repeating the process, one can converge to an intermolecular interaction that fits the experimental spectrum. However, there are problems with this approach: In the first place, it is known that a reliable surface for interacting molecules requires very many parameters; second, the number of lines measured is usually too small to establish all parameters unambiguously; and finally the solution of the rovibrational problem with a realistic surface is so expensive that one cannot afford many cycles in the iterative procedure. Thus there is a great need for computational methods that establish reliably at least some of the parameters.

The present paper describes a method to compute surfaces accurately in the asymptotic region where intermolecular overlap is negligible. Our approach starts with the computation of frequency-dependent polarizabilities as a function of $i\omega$, after which we obtain dispersion coefficients very simply via the Casimir–Polder relation.⁵

At the coupled Hartree–Fock level of theory one obtains isotropic second-order time-dependent properties of reasonable quality for both closed-shell and high-spin states.^{6,7} Errors in the isotropic polarizabilities and dispersion coefficients are on the order of 10%. Errors in the corresponding anisotropic values may be much larger, however, and are very basis set dependent. For instance, the finite field SCF (self-consistent field) method in a moderate size basis applied to NH₃ gives the wrong sign for the anisotropy of the dipole polarizability.⁸ So, already at the SCF level large basis sets are required.

One can improve the results by considering the effects of electron correlation. Several of the existing electronic correlation methods have been extended so that they can be applied to the evaluation of linear response functions.

We mention the multiconfigurational self-consistent field (MCSCF), the coupled cluster, and the many-body perturbation theory (MBPT) method. Olsen and Jørgensen⁹ formulated an MCSCF linear response theory, which has been implemented as an extension to the SIRIUS program.^{10,11} Equations for MCSCF quadratic response properties were derived a few years ago⁹ and have very recently been implemented as an addition to SIRIUS.¹² Dalgaard and Monkhorst¹³ have derived equations for the coupled cluster method, as have Koch and Jørgensen.¹⁴ Wormer and Rijks¹⁵ formulated an MBPT method for molecules in the presence of a monochromatic electric field. Their method resembles the recent method of Rice and Handy,¹⁶ who considered a Møller–Plesset second-order (MP2) quasienery of a molecule perturbed by two fields: a static and a monochromatic (time-dependent) one.

In this paper we give an improved derivation of the work of Ref. 15, which is based on a double perturbation theory with the electron correlation operator and a time-dependent external field simultaneously perturbing the time-independent Hartree–Fock reference state. Second-order correlation terms that are not accounted for by the time-independent coupled Hartree–Fock (TDCHF) method (the so-called “true correlation” terms¹⁷) are computed and added to the TDCHF values (which include only “apparent correlation”). This derivation will show that the difference between true and apparent correlation is not as clear cut as it is often thought to be. Some Pauli exclusion principle violating (EPV) diagrams can be classified both as true and apparent.

Our approach is aimed at polarizabilities on the imaginary axis and will not give the correct global characteristics of these functions on the real axis, since we introduce a double set of poles: TDCHF and MBPT poles. The latter are simply static orbital energy differences. Here we differ from Rice and Handy,¹⁶ who designed their method such that they only obtain TDCHF poles.

We will present the final formulas in a computationally tractable form and show that the evaluation of most of the terms scales with the number of orbitals as n^5 ; only a few terms scale as n^6 . Since very large basis sets are needed for the properties that we are interested in, the dependence on

n is an important factor in the success of any correlation method.

In Sec. III we will discuss briefly an alternative derivation of our theory for the static case. This derivation will show that our method can be looked upon as a generalization of a static procedure consisting of the following steps: (i) Compute the finite-field SCF multipole polarizability. (ii) Compute the second-order correlation contributions to the expectation value of the appropriate multipole moment (the first-order contribution is zero). Use for that purpose orbitals that are first-order in the external field. (iii) Differentiate this correlation contribution with respect to the external field. (iv) Add the result of (i) and (iii).

In Sec. V we give numerical results for the calculation of the frequency-dependent polarizabilities of ammonia, water, and argon, and from these we compute the van der Waals coefficients for the complexes $\text{H}_2\text{O}-\text{H}_2\text{O}$ and $\text{Ar}-\text{NH}_3$. We have chosen to study water because of the importance of the water-water interaction for practically all branches of science. The $\text{Ar}-\text{NH}_3$ system was chosen because of the rovibrational spectra recently measured in Berkeley¹ and in Nijmegen.^{2,3}

Dispersion forces in the water dimer were studied very recently by Rybak, Jeziorski, and Szalewicz¹⁸ with a method that is remotely related to ours. One of the main differences is that the present work is based on the multipole ($1/R$) expansion of the potential, which Rybak *et al.* do not employ. Use of the multipole expansion makes the calculations considerably cheaper since the monomers can be considered separately. Thus we can afford much larger atomic orbital basis sets and higher-order correlation effects. Our two monomers are simultaneously correlated through second order in the Møller-Plesset correlation potential and to infinite order in the TDCHF bubble diagrams and we have g orbitals in our bases. Furthermore, we obtain surfaces as expansions in known angular functions, which is very convenient in further applications of the potential. On the other hand, the major problem with the multipole expansion is well known: It diverges in the region of non-negligible overlap and there is no well-established prescription to damp it in this region. Also in the long range it is not always evident how many terms must be included, we stop usually at R^{-10} terms, because higher dispersion terms require at least $l=5$ orbitals for a reliable description. Note, however, that such a polarization basis is also necessary in supermolecule calculations if the correct asymptotic limit is required.

II. MBPT FREQUENCY-DEPENDENT POLARIZABILITIES

In this section we present our formulas for correlation corrections to the frequency dependent polarizability. Our derivation is based on double perturbation theory with a time dependent and a time-independent perturbation. The latter is the correlation potential V_N in normal product form with respect to the Fermi vacuum.^{19,20} The zeroth-order operator is the Fock operator F_N of the time-independent problem, so that in a hole-particle formalism the unperturbed problem reads,

$$F_N|\phi^{(0,0)}\rangle = E^{(0,0)}|\phi^{(0,0)}\rangle. \quad (1)$$

We follow the perturbation theory of Langhoff, Epstein, and Karplus²¹ in treating the time-dependent perturbation and consider arbitrary multipoles $Q_m^l = \sum_{\alpha} Z_{\alpha} S_m^l(\mathbf{r}_{\alpha})$. The function $S_m^l(\mathbf{r}_{\alpha})$ is a real solid harmonic, normalized to $4\pi/(2l+1)$, which depends on the coordinate \mathbf{r}_{α} of point charge Z_{α} . We hit the molecule by a monochromatic multipolar wave

$$H^{(1)}(t) = \frac{1}{2}W(e^{i\omega t} + e^{-i\omega t}), \quad (2)$$

where

$$W := F_m^l Q_m^l = W_N + \langle \phi^{(0,0)} | F_m^l Q_m^l | \phi^{(0,0)} \rangle \quad (3)$$

and F_m^l is the field strength. We may rewrite the time-dependent Schrödinger equation by making the ansatz²¹

$$|\Psi(t)\rangle = e^{-iE^{(0,0)}t} a(t) |\phi(t)\rangle. \quad (4)$$

It is easily shown²¹ that

$$a(t) = \frac{e^{-iR(t)t}}{\langle \phi(t) | \phi(t) \rangle^{1/2}}, \quad (5)$$

where $R(t)$ is a real function. Since it appears as a phase it does not concern us any further. The Schrödinger equation gets the form of an eigenvalue equation

$$\left[H - i \frac{d}{dt} \right] |\phi(t)\rangle = \Delta E(t) |\phi(t)\rangle$$

$$\text{with } H = F_N + V_N + H^{(1)}(t). \quad (6)$$

The quasienergy is given by

$$\Delta E(t) = \langle \phi^{(0,0)} | H | \phi(t) \rangle. \quad (7)$$

The exact wave function is expanded in a double perturbation series, which through first-order in W_N and infinite order in V_N reads

$$\phi(t) = \sum_{k=0}^{\infty} [\phi^{(k,0)} + \phi^{(k,1)}(\omega)e^{i\omega t} + \phi^{(k,1)}(-\omega)e^{-i\omega t}]. \quad (8)$$

The intermediate normalization condition

$$\langle \phi^{(0,0)} | \phi^{(k,l)} \rangle = \delta_{k,0} \delta_{l,0} \quad (9)$$

implies that we expand the perturbation corrections to the wave function in the orthogonal complement of $\phi^{(0,0)}$. Defining a resolvent on this space

$$R(\omega) := (F_N + \omega)^{-1}, \quad (10)$$

we derive easily the following corrections through second order in V_N :

$$|\phi^{(1,0)}\rangle = -R(0)V_N|\phi^{(0,0)}\rangle, \quad (11a)$$

$$|\phi^{(2,0)}\rangle = R(0)V_N R(0)V_N|\phi^{(0,0)}\rangle, \quad (11b)$$

$$|\phi^{(0,1)}(\pm\omega)\rangle = -R(\pm\omega)W_N|\phi^{(0,0)}\rangle, \quad (11c)$$

$$|\phi^{(1,1)}(\pm\omega)\rangle = -R(\pm\omega)W_N|\phi^{(1,0)}\rangle - R(\pm\omega)V_N|\phi^{(0,1)}(\pm\omega)\rangle, \quad (11d)$$

$$\begin{aligned}
|\phi^{(2,1)}(\pm\omega)\rangle &= -R(\pm\omega)W_N|\phi^{(2,0)}\rangle \\
&\quad -R(\pm\omega)V_N|\phi^{(1,1)}(\pm\omega)\rangle \\
&\quad +\Delta E^{(2,0)}R(\pm\omega)|\phi^{(0,1)}(\pm\omega)\rangle. \quad (11e)
\end{aligned}$$

Since our Hamiltonian is invariant under the substitutions $\omega \rightarrow -\omega$ and $t \rightarrow -t$, the expectation value of $Q_{m'}^{l'}$ (which we take to be in normal product form) with respect to $\Psi(t)$ is a symmetric function of ω and t . Thus the terms linear in F_m^l in this expectation value are of the form $[f(\omega) + f(-\omega)] \cos \omega t$. The factor multiplying $\cos \omega t$ is the frequency dependent $2^l-2^{l'}$ -pole polarizability $\alpha(\omega)_{m,m'}^{l,l'}$.

Numerator and denominator of the expectation value of $Q_{m'}^{l'}$ are expanded by expanding corresponding bras and kets and collecting all terms of the same perturbation order. Terms of order k in V_N and of order l in W_N are designated by $Q^{(k,l)}$ and $S^{(k,l)}$ in, respectively, the numerator and the denominator. Then

$$\begin{aligned}
\langle \Psi(t) | Q_{m'}^{l'} | \Psi(t) \rangle &= \frac{\langle \phi(t) | Q_{m'}^{l'} | \phi(t) \rangle}{\langle \phi(t) | \phi(t) \rangle} \\
&\approx \frac{Q^{(0,0)} + Q^{(1,0)} + Q^{(0,1)} + Q^{(2,0)} + Q^{(1,1)} + Q^{(2,1)}}{S^{(0,0)} + S^{(1,0)} + S^{(0,1)} + S^{(2,0)} + S^{(1,1)} + S^{(2,1)}} \\
&\approx Q^{(0,1)} + Q^{(2,0)} + Q^{(1,1)} + Q^{(2,1)} - Q^{(0,1)}S^{(2,0)}. \quad (12)
\end{aligned}$$

Noting that $S^{(0,0)} = 1$, we expanded the denominator up to and including second order in V_N and first order in W_N and used $Q^{(0,0)} = Q^{(1,0)} = S^{(1,0)} = S^{(0,1)} = 0$. In order to obtain the total expectation value of the operator we must add its Fermi vacuum expectation value, i.e., its HF contribution, to Eq. (12). The time-independent part of Eq. (12) is the usual second order correlation contribution of the permanent moment,

$$\begin{aligned}
Q^{(2,0)} &= \langle \phi^{(0,0)} | Q_{m'}^{l'} | \phi^{(2,0)} \rangle + \langle \phi^{(2,0)} | Q_{m'}^{l'} | \phi^{(0,0)} \rangle \\
&\quad + \langle \phi^{(1,0)} | Q_{m'}^{l'} | \phi^{(1,0)} \rangle. \quad (13)
\end{aligned}$$

We obtain an unlinked contribution from

$$S^{(2,0)} = \langle \phi^{(1,0)} | \phi^{(1,0)} \rangle = \langle \phi^{(0,0)} | V_N R(0)^2 V_N | \phi^{(0,0)} \rangle. \quad (14)$$

The time-dependent terms in Eq. (12) appearing with $\exp(i\omega t)$ are

$$\begin{aligned}
Q^{(0,1)} &= (\langle \phi^{(0,0)} | Q_{m'}^{l'} | \phi^{(0,1)}(\omega) \rangle \\
&\quad + \langle \phi^{(0,1)}(-\omega) | Q_{m'}^{l'} | \phi^{(0,0)} \rangle) e^{i\omega t}, \quad (15a)
\end{aligned}$$

$$\begin{aligned}
Q^{(1,1)} &= (\langle \phi^{(0,0)} | Q_{m'}^{l'} | \phi^{(1,1)}(\omega) \rangle \\
&\quad + \langle \phi^{(1,1)}(-\omega) | Q_{m'}^{l'} | \phi^{(0,0)} \rangle \\
&\quad + \langle \phi^{(1,0)} | Q_{m'}^{l'} | \phi^{(0,1)}(\omega) \rangle \\
&\quad + \langle \phi^{(0,1)}(-\omega) | Q_{m'}^{l'} | \phi^{(1,0)} \rangle) e^{i\omega t}, \quad (15b)
\end{aligned}$$

$$\begin{aligned}
Q^{(2,1)} &= (\langle \phi^{(0,0)} | Q_{m'}^{l'} | \phi^{(2,1)}(\omega) \rangle + \langle \phi^{(2,1)}(-\omega) | Q_{m'}^{l'} | \phi^{(0,0)} \rangle + \langle \phi^{(2,0)} | Q_{m'}^{l'} | \phi^{(0,1)}(\omega) \rangle + \langle \phi^{(0,1)}(-\omega) | Q_{m'}^{l'} | \phi^{(2,0)} \rangle \\
&\quad + \langle \phi^{(1,0)} | Q_{m'}^{l'} | \phi^{(1,1)}(\omega) \rangle + \langle \phi^{(1,1)}(-\omega) | Q_{m'}^{l'} | \phi^{(1,0)} \rangle) e^{i\omega t}. \quad (15c)
\end{aligned}$$

Note that the factors of $\exp(i\omega t)$ in Eq. (15) are invariant under the substitution $\omega \rightarrow -\omega$. Since the very same terms arise from Eq. (12) with $\exp(-i\omega t)$, we find that indeed the time dependence is given by $\cos \omega t$. Substitution of Eqs. (11) into expressions (15) yields the frequency dependent polarizability up to and including terms in V_N^2

$$\begin{aligned}
\alpha(\omega)_{m,m'}^{l,l'} &= \langle \phi^{(0,0)} | Q_{m'}^{l'} R(\omega) Q_m^l S^{(2,0)} + Q_{m'}^{l'} R^2(\omega) Q_m^l \Delta E^{(2,0)} - Q_{m'}^{l'} R(\omega) Q_m^l + Q_{m'}^{l'} R(\omega) V_N R(\omega) Q_m^l \\
&\quad - Q_{m'}^{l'} R(\omega) V_N R(\omega) V_N R(\omega) Q_m^l - V_N R(0) Q_{m'}^{l'} R(\omega) Q_m^l R(0) V_N + Q_{m'}^{l'} R(\omega) Q_m^l R(0) V_N \\
&\quad + V_N R(0) Q_{m'}^{l'} R(\omega) Q_m^l - V_N R(0) V_N R(0) Q_{m'}^{l'} R(\omega) Q_m^l - Q_{m'}^{l'} R(\omega) Q_m^l R(0) V_N R(0) V_N \\
&\quad - V_N R(0) Q_{m'}^{l'} R(\omega) V_N R(\omega) Q_m^l - Q_{m'}^{l'} R(\omega) V_N R(\omega) Q_m^l R(0) V_N | \phi^{(0,0)} \rangle \\
&\quad + \text{same terms with } \omega \rightarrow -\omega. \quad (16)
\end{aligned}$$

Since the Hartree-Fock ground state is real and all operators in Eq. (16) are Hermitian, the order in the operator products may be reversed.

Expression (16) contains N -electron operators. In order to reduce it to one containing only integrals over (unperturbed) molecular orbitals, different routes can be taken. One obvious route is the expression of the reduced

resolvent $R(\omega)$ in a basis of Slater determinants, followed by repeated application of the Slater-Condon rules. In our opinion a much more convenient approach proceeds by the aid of Hugenholtz/Goldstone diagrams; see Refs. 22 and 23. In these references it is shown that the unlinked terms containing the factors $\Delta E^{(2,0)}$ and $S^{(2,0)}$ cancel against the other unlinked terms arising in Eq. (16). For an outline of

the diagrammatic method one may for instance consult the work of Čížek and Paldus.¹⁹

Caves and Karplus²⁴ have shown that the TDCHF approach leads diagrammatically to an infinite summation of "bubble" diagrams. Since we are looking for a correction to TDCHF we must remove all bubble terms from Eq. (16), including the uncoupled HF polarizability $Q^{(0,1)}$. The terms of zeroth- and first-order in V_N are accounted for by TDCHF (as are a few of the second-order terms), so we omit these.

We will now list the non-TDCHF terms contributing to the symmetrized polarizability $[\alpha(i\omega)_{m,m'}^{l,l'} + \alpha(i\omega)_{m',m}^{l',l}]/2$ and to that end group the 48 different second-order (in V_N) Hugenholtz diagrams into 4 different contributions A_1, \dots, A_4 which—when summed—yield the required correction to the TDCHF polarizability. The 48 Hugenholtz diagrams together with the corresponding Goldstone versions can be found in Ref. 22. We use the convention that $i, j, k \dots$ run over occupied orbitals, $a, b, c \dots$ run over virtual orbitals, and p, q, r, \dots run over arbitrary orbitals. The corresponding spinorbitals are given by capital letters. Denominators containing differences of unperturbed orbital energies are written as $\Delta_{ai} := \epsilon_i - \epsilon_a$. We define the quantity

$$P_{ai,bj} := \frac{2(ai|bj) - (aj|bi)}{\Delta_{ai} + \Delta_{bj}}$$

Defining

$$V_{ai} := \sum_b \frac{\Delta_{bi}(\langle i|Q_m^l|b\rangle\langle b|Q_m^{l'}|a\rangle + \langle i|Q_m^{l'}|b\rangle\langle b|Q_m^l|a\rangle)}{(\Delta_{bi}^2 + \omega^2)} - \sum_j \frac{\Delta_{aj}(\langle i|Q_m^l|j\rangle\langle j|Q_m^{l'}|a\rangle + \langle i|Q_m^{l'}|j\rangle\langle j|Q_m^l|a\rangle)}{(\Delta_{aj}^2 + \omega^2)}, \quad (20)$$

we find the second contribution

$$A_2 = 4 \sum_{ai} \left[\sum_{cbj} (ac|bj)P_{ci,bj} - \sum_{kjb} (ki|bj)P_{ak,bj} \right] \frac{V_{ai}}{\Delta_{ai}}. \quad (21)$$

This is an n^5 term.

The following auxiliary quantities can be evaluated by n^5 algorithms:

$$T_{jk} := \sum_{abi} \frac{(ai|bk)[2(ai|bj) - (aj|bi)]}{\Delta_{ai} + \Delta_{bj}}, \quad (22a)$$

$$T'_{jk} := \sum_{abi} \frac{(ai|bk)[2(ai|bj) - (aj|bi)]}{(\Delta_{ai} + \Delta_{bj})(\Delta_{ai} + \Delta_{bk})}, \quad (22b)$$

$$S_{bc} := \sum_{aij} \frac{(ai|cj)[2(ai|bj) - (aj|bi)]}{\Delta_{ai} + \Delta_{bj}}, \quad (22c)$$

$$S'_{bc} := \sum_{aij} \frac{(ai|cj)[2(ai|bj) - (aj|bi)]}{(\Delta_{ai} + \Delta_{bj})(\Delta_{ai} + \Delta_{cj})}. \quad (22d)$$

In terms of these the third contribution is,

with

$$(pq|rs) := \left\langle p(1)r(2) \left| \frac{1}{r_{12}} \right| q(1)s(2) \right\rangle \quad (17)$$

and the matrix

$$F_{ai,bj} := - \sum_{ck} [(bc|ki)P_{ak,cj} + (bi|kc)P_{aj,ck} + (ac|kj)P_{bk,ci} + (aj|kc)P_{bi,ck}] + \sum_{kl} (ki|lj)P_{ak,bl} + \sum_{cd} (ac|bd)P_{ci,dj}. \quad (18)$$

Note that it takes n^6 operations to compute the matrix F , but note also that the matrix is independent of the multipoles and the frequency ω , so that it has to be calculated only once. This is indeed a great saving. For instance, in the case of the water dimer, where we calculate dispersion coefficients through C_{10} , we need 66 different H_2O polarizabilities at 11 frequencies.

The first contribution is then

$$A_1 = 4 \sum_{aibj} F_{ai,bj} \times \frac{\Delta_{bj}(\langle i|Q_m^l|a\rangle\langle j|Q_m^{l'}|b\rangle + \langle i|Q_m^{l'}|a\rangle\langle j|Q_m^l|b\rangle)}{(\Delta_{bj}^2 + \omega^2)(\Delta_{ai} + \Delta_{bj})}. \quad (19)$$

$$A_3 = -2 \sum_{cjk} \left[\frac{\langle j | Q'_m | c \rangle \langle c | Q'_m | k \rangle + \langle j | Q'_m | c \rangle \langle c | Q'_m | k \rangle}{\Delta_{cj}^2 + \omega^2} \left\{ T_{jk} \frac{\Delta_{cj} \Delta_{ck} - \omega^2}{\Delta_{ck}^2 + \omega^2} + T'_{jk} \Delta_{cj} \right\} \right] \\ - 2 \sum_{bck} \left[\frac{\langle c | Q'_m | k \rangle \langle k | Q'_m | b \rangle + \langle c | Q'_m | k \rangle \langle k | Q'_m | b \rangle}{\Delta_{bk}^2 + \omega^2} \left\{ S_{bc} \frac{\Delta_{bk} \Delta_{ck} - \omega^2}{\Delta_{ck}^2 + \omega^2} + S'_{bc} \Delta_{bk} \right\} \right]. \quad (23)$$

The last contribution is written in terms of the following vectors indexed by $(a,i) \leq (b,j)$. As a matter of fact these vectors are wave functions that are first order, both in the correlation and in the external field. (See Fig. 1 for their diagrammatic representation.) Their evaluation is an n^5 process,

$$g'_m := \begin{cases} - \sum_k \left[\frac{\langle k | Q'_m | j \rangle (ai | bk) + \langle k | Q'_m | i \rangle (ak | bj)}{\Delta_{ai} + \Delta_{bk}} \right] & \text{if } (a,i) \neq (b,j), \\ - \sqrt{2} \sum_k \left[\frac{\langle k | Q'_m | i \rangle (ai | ak)}{\Delta_{ai} + \Delta_{ak}} \right] & \text{otherwise;} \end{cases} \quad (24)$$

$$f'_m := \begin{cases} \sum_c \left[\frac{\langle b | Q'_m | c \rangle (ai | cj) + \langle a | Q'_m | c \rangle (bj | ci)}{\Delta_{ai} + \Delta_{cj}} \right] & \text{if } (a,i) \neq (b,j), \\ \sqrt{2} \sum_c \left[\frac{\langle a | Q'_m | c \rangle (ai | ci)}{\Delta_{ai} + \Delta_{ci}} \right] & \text{otherwise;} \end{cases} \quad (25)$$

$$u'_m := \begin{cases} - \sum_k \left[\frac{\Delta_{bk}}{\Delta_{bk}^2 + \omega^2} \langle b | Q'_m | k \rangle (ai | kj) + \frac{\Delta_{ak}}{\Delta_{ak}^2 + \omega^2} \langle a | Q'_m | k \rangle (bj | ki) \right] & \text{if } (a,i) \neq (b,j), \\ - \sqrt{2} \sum_k \left[\frac{\Delta_{ak}}{\Delta_{ak}^2 + \omega^2} \langle a | Q'_m | k \rangle (ai | ki) \right] & \text{otherwise;} \end{cases} \quad (26)$$

$$v'_m := \begin{cases} - \sum_k \left[\frac{\omega}{\Delta_{bk}^2 + \omega^2} \langle b | Q'_m | k \rangle (ai | kj) + \frac{\omega}{\Delta_{ak}^2 + \omega^2} \langle a | Q'_m | k \rangle (bj | ki) \right] & \text{if } (a,i) \neq (b,j), \\ - \sqrt{2} \sum_k \left[\frac{\omega}{\Delta_{ak}^2 + \omega^2} \langle a | Q'_m | k \rangle (ai | ki) \right] & \text{otherwise;} \end{cases} \quad (27)$$

$$x'_m := \begin{cases} \sum_c \left[\frac{\Delta_{cj}}{\Delta_{cj}^2 + \omega^2} \langle c | Q'_m | j \rangle (ai | bc) + \frac{\Delta_{ci}}{\Delta_{ci}^2 + \omega^2} \langle c | Q'_m | i \rangle (bj | ac) \right] & \text{if } (a,i) \neq (b,j), \\ \sqrt{2} \sum_c \left[\frac{\Delta_{ci}}{\Delta_{ci}^2 + \omega^2} \langle c | Q'_m | i \rangle (ai | ac) \right] & \text{otherwise;} \end{cases} \quad (28)$$

$$y'_m := \begin{cases} \sum_c \left[\frac{\omega}{\Delta_{cj}^2 + \omega^2} \langle c | Q'_m | j \rangle (ai | bc) + \frac{\omega}{\Delta_{ci}^2 + \omega^2} \langle c | Q'_m | i \rangle (bj | ac) \right] & \text{if } (a,i) \neq (b,j), \\ \sqrt{2} \sum_c \left[\frac{\omega}{\Delta_{ci}^2 + \omega^2} \langle c | Q'_m | i \rangle (ai | ac) \right] & \text{otherwise.} \end{cases} \quad (29)$$

In order to present concisely the contribution from these vectors, we define the following weighted contractions:

$$t \cdot s := \sum_{(a,i) > (b,j)} \frac{\Delta_{ai} + \Delta_{bj}}{(\Delta_{ai} + \Delta_{bj})^2 + \omega^2} t_{ai;bj} s_{ai;bj}, \quad (30a)$$

$$t \circ s := \sum_{(a,i) > (b,j)} - \frac{\omega}{(\Delta_{ai} + \Delta_{bj})^2 + \omega^2} t_{ai;bj} s_{ai;bj}, \quad (30b)$$

$$t \cdot \tilde{s} := \sum_{(a,i) > (b,j)} \frac{\Delta_{ai} + \Delta_{bj}}{(\Delta_{ai} + \Delta_{bj})^2 + \omega^2} t_{ai;bj} s_{aj;bi}, \quad (30c)$$

$$t \circ \tilde{s} := \sum_{(a,i) > (b,j)} - \frac{\omega}{(\Delta_{ai} + \Delta_{bj})^2 + \omega^2} t_{ai;bj} s_{aj;bi}, \quad (30d)$$

so that the final contribution to the symmetrized polarizability can be written as

$$\begin{aligned}
 A_4 = & 4[2(\mathbf{f}'_{m'} + \mathbf{g}'_{m'}) \cdot (\mathbf{f}'_m + \mathbf{g}'_m) - (\mathbf{f}'_{m'} + \mathbf{g}'_{m'}) \cdot (\tilde{\mathbf{f}}'_m + \tilde{\mathbf{g}}'_m)] + 4[2(\mathbf{u}'_{m'} + \mathbf{x}'_{m'}) \cdot (\mathbf{f}'_m + \mathbf{g}'_m) - (\mathbf{u}'_{m'} + \mathbf{x}'_{m'}) \cdot (\tilde{\mathbf{f}}'_m + \tilde{\mathbf{g}}'_m)] \\
 & + 4[2(\mathbf{u}'_m + \mathbf{x}'_m) \cdot (\mathbf{f}'_{m'} + \mathbf{g}'_{m'}) - (\mathbf{u}'_m + \mathbf{x}'_m) \cdot (\tilde{\mathbf{f}}'_{m'} + \tilde{\mathbf{g}}'_{m'})] + 4[2(\mathbf{u}'_{m'} + \mathbf{x}'_{m'}) \cdot (\mathbf{u}'_m + \mathbf{x}'_m) - (\mathbf{u}'_{m'} + \mathbf{x}'_{m'}) \cdot (\tilde{\mathbf{u}}'_m + \tilde{\mathbf{x}}'_m)] \\
 & - 4[2(\mathbf{v}'_{m'} + \mathbf{y}'_{m'}) \cdot (\mathbf{v}'_m + \mathbf{y}'_m) - (\mathbf{v}'_{m'} + \mathbf{y}'_{m'}) \cdot (\tilde{\mathbf{v}}'_m + \tilde{\mathbf{y}}'_m)] + 4[2(\mathbf{v}'_{m'} + \mathbf{y}'_{m'}) \circ (\mathbf{f}'_m + \mathbf{g}'_m) - (\mathbf{v}'_{m'} + \mathbf{y}'_{m'}) \circ (\tilde{\mathbf{f}}'_m + \tilde{\mathbf{g}}'_m)] \\
 & + 4[2(\mathbf{v}'_m + \mathbf{y}'_m) \circ (\mathbf{f}'_{m'} + \mathbf{g}'_{m'}) - (\mathbf{v}'_m + \mathbf{y}'_m) \circ (\tilde{\mathbf{f}}'_{m'} + \tilde{\mathbf{g}}'_{m'})] + 4[2(\mathbf{u}'_{m'} + \mathbf{x}'_{m'}) \circ (\mathbf{v}'_m + \mathbf{y}'_m) - (\mathbf{u}'_{m'} + \mathbf{x}'_{m'}) \circ (\tilde{\mathbf{v}}'_m + \tilde{\mathbf{y}}'_m)] \\
 & + 4[2(\mathbf{u}'_m + \mathbf{x}'_m) \circ (\mathbf{v}'_{m'} + \mathbf{y}'_{m'}) - (\mathbf{u}'_m + \mathbf{x}'_m) \circ (\tilde{\mathbf{v}}'_{m'} + \tilde{\mathbf{y}}'_{m'})]. \tag{31}
 \end{aligned}$$

The evaluation of these contractions is an n^4 algorithm.

It may be observed that in the equations for A_1 to A_4 the summations are unrestricted, i.e., the fact is not taken into account that the spin orbitals occur only once in every bra and ket when the resolvent $R(\omega)$ is expressed in a basis of Slater determinants. We seem to include contributions from EPV diagrams. However, at this point there is a indeterminacy in the theory. In a consistent MBPT formalism *all* EPV diagrams cancel mutually, whereas in the diagrammatic analysis of the TDCHF method²⁴ some EPV diagrams *do* appear. So it is debatable whether we must include the EPV terms that arise from bubble diagrams. This point is exemplified in Fig. 2, where we find some apparent correlation diagrams side by side with closely related true correlation diagrams.¹⁷ Also the overall sign $(-)^{l+h}$ of the Goldstone diagrams is shown (the number

of hole lines $h=3$ is odd in the cases of Fig. 2, the number of closed loops l varies). If we take $K=I$ in both sets of diagrams, we see that they cancel each other. This exhibits two points: (i) EPV true and apparent correlation diagrams are undistinguishable, and (ii) if we take the above formulas as they stand, the second-order EPV TDCHF terms will be canceled. In the next section we will give a derivation that also yields this cancellation, but since the theory is undetermined, we will study this point from the numerical point of view. We therefore present the formulas for the second-order EPV bubble diagrams.

With the auxiliary quantity

$$\begin{aligned}
 G_{aci} = & \sum_{bj} \left\{ \frac{[2(ai|jb) - (ab|ji)](ci|bj)}{\Delta_{bj} + \Delta_{ci}} \right. \\
 & \left. + \frac{[(ab|ji) - (ai|jb)](bi|cj)}{\Delta_{bj} + \Delta_{ci}} \right\} \tag{32}
 \end{aligned}$$

the first bubble EPV contribution can be written as

$$\begin{aligned}
 B_1 = & 4 \sum_{iac} G_{aci} \langle i | Q'_m | a \rangle \langle i | Q''_m | c \rangle \\
 & + \langle i | Q''_m | a \rangle \langle i | Q'_m | c \rangle \frac{\Delta_{ai}\Delta_{ci} + \omega^2}{(\Delta_{ai}^2 + \omega^2)(\Delta_{ci}^2 + \omega^2)}. \tag{33}
 \end{aligned}$$

Define

$$\begin{aligned}
 G'_{aik} = & \sum_{bj} \left\{ \frac{[2(ak|jb) - (ab|kj)](ai|bj)}{\Delta_{bj} + \Delta_{ai}} \right. \\
 & \left. + \frac{[(ab|kj) - (ak|jb)](aj|bi)}{\Delta_{bj} + \Delta_{ai}} \right\}, \tag{34}
 \end{aligned}$$

then the second bubble EPV contribution is,

$$\begin{aligned}
 B_2 = & 4 \sum_{ika} G'_{aik} \langle i | Q'_m | a \rangle \langle k | Q''_m | a \rangle \\
 & + \langle i | Q''_m | a \rangle \langle k | Q'_m | a \rangle \frac{\Delta_{ai}\Delta_{ak} + \omega^2}{(\Delta_{ai}^2 + \omega^2)(\Delta_{ak}^2 + \omega^2)}. \tag{35}
 \end{aligned}$$

The restriction in the sum (35) is due to the fact that some EPV terms would be accounted for twice if both sums (34) and (35) would run freely. This can happen for the terms

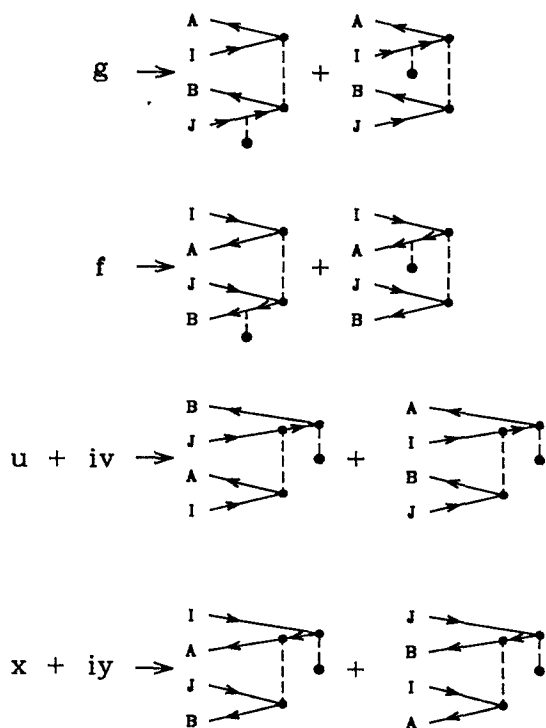


FIG. 1. Goldstone diagrams representing the first-order correlated, first-order externally perturbed wave functions of Eqs. (24)–(29). The interaction with the external field is represented by a crossed circle. The denominators to the left of this one-particle vertex are ω dependent.

with $a=c$ and $i=k$. Since these terms are already taken into account in sum (34), they are explicitly excluded in sum (35). Defining

$$Q_{ai,bj} = \frac{(ai|bj)}{\Delta_{ai} + \Delta_{bj}} \quad (36)$$

and

$$F_{ika}^{p1} = \sum_{jb} \{ [2(bj|ak) - (bk|aj)] Q_{ai,bj} + [(bk|aj) - (bj|ak)] Q_{aj,bi} \},$$

$$F_{ika}^{p2} = \sum_{jb} \frac{1}{(\Delta_{bj} + \Delta_{ak})} \{ [2(bj|ak) - (bk|aj)] Q_{ai,bj} + [(bk|aj) - (bj|ak)] Q_{aj,bi} \}, \quad (37)$$

we may write the third bubble EPV contribution as

$$B_3 = 2 \sum_{\substack{ika \\ i \neq k}} [\langle i | Q_m^l | a \rangle \langle a | Q_{m'}^{l'} | k \rangle + \langle i | Q_{m'}^{l'} | a \rangle \langle a | Q_m^l | k \rangle]$$

$$\times \left[\frac{1}{(\Delta_{ai}^2 + \omega^2)} \left(\frac{\Delta_{ai} \Delta_{ak} - \omega^2}{\Delta_{ak}^2 + \omega^2} F_{ika}^{p1} + \Delta_{ai} F_{ika}^{p2} \right) \right]. \quad (38)$$

Define finally

$$F_{iac}^{h1} = \sum_{jb} \{ [2(ci|bj) - (cj|bi)] Q_{ai,bj} + [(bi|cj) - (ci|bj)] Q_{aj,bi} \},$$

$$F_{iac}^{h2} = \sum_{jb} \frac{1}{(\Delta_{bj} + \Delta_{ci})} \{ [2(ci|bj) - (cj|bi)] Q_{ai,bj} + [(bi|cj) - (ci|bj)] Q_{aj,bi} \}, \quad (39)$$

then the last bubble EPV becomes

$$B_4 = 2 \sum_{iac} [\langle c | Q_m^l | i \rangle \langle i | Q_{m'}^{l'} | a \rangle + \langle c | Q_{m'}^{l'} | i \rangle \langle i | Q_m^l | a \rangle]$$

$$\times \left[\frac{1}{(\Delta_{ai}^2 + \omega^2)} \left(\frac{\Delta_{ai} \Delta_{ci} - \omega^2}{\Delta_{ci}^2 + \omega^2} F_{iac}^{h1} + \Delta_{ai} F_{iac}^{h2} \right) \right]. \quad (40)$$

Again we need to be careful not to take into account some of the EPV terms twice. Hence there is a correction in Eq. (38), where we restrict the sum by imposing $i \neq k$.

To end this section we point out that in the earlier results of Rijks *et al.*^{22,23} the terms B_1, \dots, B_4 have been included.

III. STATIC DOUBLE PERTURBATION THEORY

In order to put our method in a different perspective and to relate it to existing procedures for calculating static polarizabilities, we sketch an alternative derivation for the special case $\omega=0$. The time-independent analysis of this section will be based on uncoupled HF orbitals, but could equally well be given in terms of coupled HF orbitals. The use of coupled HF orbitals is tantamount to "dressing" the one-electron interaction with an infinite series of RPA-type correlation diagrams.¹⁷ Since the dressed one-electron in-

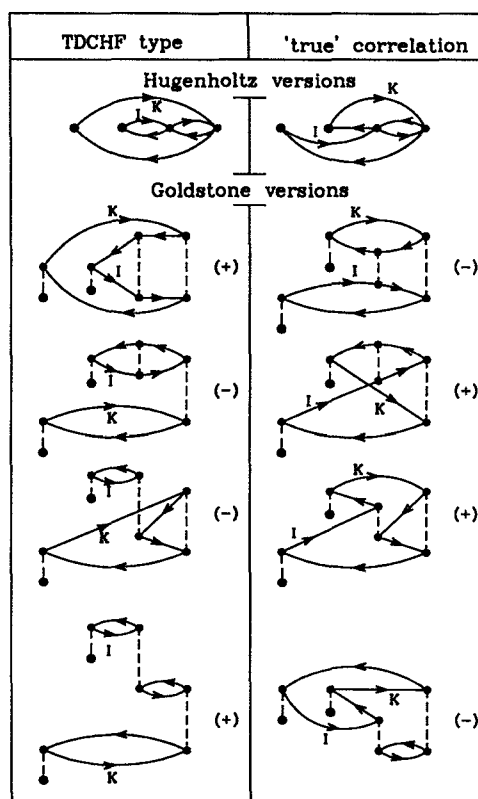


FIG. 2. An example of true and apparent correlation diagrams that become undistinguishable when they are EPV, i.e., if $I=K$. In that case the two diagrams cancel mutually.

teraction is linear in the field the discussion of this section holds equally well for coupled HF orbitals. However, we have chosen to use the "bare" interaction in the discussion because our computational method is based on it. It is possible to extend the formalism of Sec. II to coupled HF orbitals, but this would increase the cost of the calculations considerably, since the one-electron interactions are then ω dependent. We first observe that for $\omega=0$ our perturbation theory becomes ordinary Rayleigh–Schrödinger perturbation theory (RSPT), so that we may use the usual RSPT expressions. Quite generally we may define a first order static multipole moment as the first derivative of the exact energy of the system (in the field $F_m^l Q_m^l$) at $F_m^l=0$,

$$\mathcal{M}_m^l = \left[\frac{\partial E(F_m^l)}{\partial F_m^l} \right]_{F_m^l=0}. \quad (41)$$

If we separate the energy into a Hartree–Fock energy plus a correlation contribution, \mathcal{M}_m^l is split likewise in a Hartree–Fock and a correlation part. We will consider finite-field SCF and we recall that in the static case TDCHF is the same as finite-field SCF.

In order to find the correlation contribution to the moments \mathcal{M}_m^l we start from the approximate Møller–Plesset second order (MP2) correlation energy

$$E_{MP2} = \langle \phi^{(0)} | VR(0) V | \phi^{(0)} \rangle, \quad (42)$$

where $\phi^{(0)}$ is of zeroth order in V_N and, in principle, of infinite order in W_N . Consider arbitrary spin orbitals P and Q with corresponding orbital energies, both perturbed up to first order in W_N

$$\begin{aligned} {}^1\epsilon_P &= \epsilon_P + F'_m \langle P | Q'_m | P \rangle, \\ |{}^1P\rangle &= |P\rangle + F'_m \sum_{Q \neq P} |Q\rangle \frac{\langle Q | Q'_m | P \rangle}{\Delta_{QP}}. \end{aligned} \quad (43)$$

The quantities not preceded by a superscript are of zeroth order in W_N . The MP2 energy in terms of these uncoupled Hartree-Fock quantities is

$$E_{\text{MP2}}(F'_m) = \frac{1}{4} \sum_{I,J,A,B} \frac{\langle I^1 J^1 | A^1 B^1 \rangle \langle I^1 A^1 B^1 | I^1 J^1 \rangle}{\Delta_{AI} + \Delta_{BJ}}, \quad (44)$$

where

$$\begin{aligned} \langle PQ || RS \rangle &= \langle P(1)Q(2) | r_{12}^{-1} | R(1)S(2) \rangle \\ &\quad - \langle P(1)Q(2) | r_{12}^{-1} | S(1)R(2) \rangle \end{aligned} \quad (45)$$

and

$${}^1\Delta_{AI} = {}^1\epsilon_I - {}^1\epsilon_A. \quad (46)$$

With orbitals perturbed to first order the numerator of the MP2 energy is of eighth order in the field, but is, of course, incomplete as higher than first-order contributions from the orbitals are lacking. Under differentiation of E_{MP2} with respect to the field at $F'_m = 0$, only the terms survive that are first order in the field. The expansion of the denominator to first order is

$$\frac{1}{\Delta_{AI} + \Delta_{BJ}} = \frac{1}{\Delta_{AI} + \Delta_{BJ}} + F'_m \frac{\langle A | Q'_m | A \rangle + \langle B | Q'_m | B \rangle - \langle I | Q'_m | I \rangle - \langle J | Q'_m | J \rangle}{(\Delta_{AI} + \Delta_{BJ})^2}. \quad (47)$$

If we substitute Eq. (43) into Eq. (44) two kinds of first-order terms are obtained: The first kind arises from the first-order terms in the numerator and the zeroth-order terms in the denominator of Eq. (44). The second kind consists of the zeroth-order numerator terms multiplied by the first-order terms of Eq. (47). All the terms of the second kind will cancel against some terms of the first kind. In order to clarify this, we consider temporarily only terms due to the substitution of ${}^1|I\rangle$. If the sum in this orbital is split into one over occupied and virtual orbitals, we get as terms of the first kind

$$\begin{aligned} &+ \frac{1}{4} F'_m \sum_{\substack{I,J,K,A,B \\ (K \neq I)}} \frac{\langle I | Q'_m | K \rangle \langle KJ || AB \rangle \langle AB || IJ \rangle + \langle IJ || AB \rangle \langle AB || KJ \rangle \langle K | Q'_m | I \rangle}{\Delta_{KI} (\Delta_{AI} + \Delta_{BJ})} \\ &+ \frac{1}{4} F'_m \sum_{I,J,A,B,C} \frac{\langle I | Q'_m | C \rangle \langle CJ || AB \rangle \langle AB || IJ \rangle + \langle IJ || AB \rangle \langle AB || CJ \rangle \langle C | Q'_m | I \rangle}{\Delta_{CI} (\Delta_{AI} + \Delta_{BJ})}. \end{aligned} \quad (48)$$

We rewrite the first term of Eq. (48)

$$\begin{aligned} &= + \frac{1}{4} F'_m \sum_{\substack{I,J,K,A,B \\ (I \neq K)}} \langle I | Q'_m | K \rangle \langle KJ || AB \rangle \langle AB || IJ \rangle \left[\frac{1}{\Delta_{KI}} \left(\frac{1}{\Delta_{AI} + \Delta_{BJ}} - \frac{1}{\Delta_{AK} + \Delta_{BJ}} \right) \right] \\ &= - \frac{1}{4} F'_m \sum_{\substack{I,J,K,A,B \\ (I \neq K)}} \langle I | Q'_m | K \rangle \langle KJ || AB \rangle \langle AB || IJ \rangle \left(\frac{1}{(\Delta_{AI} + \Delta_{BJ})(\Delta_{AK} + \Delta_{BJ})} \right) \\ &= - \frac{1}{4} F'_m \sum_{I,J,K,A,B} \frac{\langle I | Q'_m | K \rangle \langle KJ || AB \rangle \langle AB || IJ \rangle}{(\Delta_{AI} + \Delta_{BJ})(\Delta_{AK} + \Delta_{BJ})} + \frac{1}{4} F'_m \sum_{I,J,A,B} \frac{\langle I | Q'_m | I \rangle \langle IJ || AB \rangle \langle AB || IJ \rangle}{(\Delta_{AI} + \Delta_{BJ})^2}. \end{aligned} \quad (49)$$

The very last term of Eq. (49) cancels against the term containing $\langle I | Q'_m | I \rangle$ that occurs among the terms of the second kind. In the same way, the restrictions in the expansions of the orbitals ${}^1|J\rangle$, ${}^1|A\rangle$, and ${}^1|B\rangle$ lead to cancellations against terms of the second kind.

The expression for the MP2 contribution to the moment \mathcal{M}'_m becomes then

$$\begin{aligned} (\mathcal{M}'_m)_{\text{MP2}} \equiv Q^{(2,0)} &= -\frac{1}{2} \sum_{I,J,K,A,B} \frac{\langle KJ || AB \rangle \langle I | Q'_m | K \rangle \langle AB || IJ \rangle}{(\Delta_{AI} + \Delta_{BJ})(\Delta_{AK} + \Delta_{BJ})} + \frac{1}{2} \sum_{I,J,A,B,C} \frac{\langle C | Q'_m | I \rangle \langle AB || CJ \rangle \langle IJ || AB \rangle}{\Delta_{CI} (\Delta_{AI} + \Delta_{BJ})} \\ &\quad - \frac{1}{2} \sum_{I,J,K,A,B} \frac{\langle A | Q'_m | K \rangle \langle KB || IJ \rangle \langle IJ || AB \rangle}{\Delta_{AK} (\Delta_{AI} + \Delta_{BJ})} + \frac{1}{2} \sum_{I,J,A,B,C} \frac{\langle IJ || CB \rangle \langle C | Q'_m | A \rangle \langle AB || IJ \rangle}{(\Delta_{AI} + \Delta_{BJ})(\Delta_{CI} + \Delta_{BJ})}. \end{aligned} \quad (50)$$

The diagrams corresponding to this expression are given in Fig. 3 and are the same as those given by Sadlej.¹⁷ Although the MP2 energy is derived from a wave function that is first order in V_N , differentiation gives all the second-order (in V_N) contributions to the multipole moment. This also means that the following equality holds through V_N^2 , cf. Eqs. (13) and (41):

$$\left[\frac{\partial E_{\text{MP2}}(F_m^l)}{\partial F_m^l} \right]_{F_m^l=0} = \langle \phi^{(0,0)} + \phi^{(1,0)} + \phi^{(2,0)} | \mathcal{Q}_m^l | \phi^{(0,0)} + \phi^{(1,0)} + \phi^{(2,0)} \rangle, \quad (51)$$

so, the Hellmann–Feynman theorem is satisfied up to and including second order in the correlation.

We will present values for the correlated multipole moments, which can be evaluated by n^5 algorithms. We have used the following formulas:

$$F_{ik}^h = -2 \sum_{jab} \frac{(ai|bj)}{\Delta_{ai} + \Delta_{bj}} P_{ak,bj},$$

$$F_{ca}^p = 2 \sum_{ijb} \frac{(ai|bj)}{\Delta_{ai} + \Delta_{bj}} P_{bj,ci}, \quad (52)$$

$$F_{ai}^{ph} = -2 \sum_{jkb} \frac{(bk|ij)}{\Delta_{ai}} P_{c_j,bk} + 2 \sum_{jbc} \frac{(ba|cj)}{\Delta_{ai}} P_{bi,cj},$$

where $P_{ai,bj}$ is defined by Eq. (17). The multipole moment in terms of these quantities is

$$(\mathcal{M}_m^l)_{\text{MP2}} = \sum_{ik} F_{ik}^h \langle i | \mathcal{Q}_m^l | k \rangle + \sum_{ca} F_{ca}^p \langle c | \mathcal{Q}_m^l | a \rangle + 2 \sum_{ai} F_{ai}^{ph} \langle a | \mathcal{Q}_m^l | i \rangle. \quad (53)$$

Returning now to polarizabilities, we start from the expression for $(\mathcal{M}_m^l)_{\text{MP2}}$ given in Eq. (50), substitute the uncoupled HF orbitals of Eq. (43), and differentiate the moment to the external field. This yields the correlation correction to be added to the finite-field SCF value of the static polarizability,

$$\alpha_{m,m'}^{l,l'} = \left[\frac{\partial [\mathcal{M}_m^l (F_m^l)^{l'}]_{\text{MP2}}}{\partial F_m^l} \right]_{F_m^l=0}. \quad (54)$$

We worked out all the nonvanishing terms of Eq. (54), wrote them down diagrammatically, and found that they are exactly the static forms of the 48 Hugenholtz diagrams which arose from Eq. (16). In order to test our program we used Eq. (54) by differentiating numerically Eq. (50).

Note finally that the Pauli principle does not play a role in the derivations of this section. The MP2 energy, written in terms of antisymmetric integrals, satisfies the exclusion principle and also the orbital expansions do not violate this principle. So, the derivation of this section suggest that we correct the finite-field SCF values by A_1, \dots, A_4 of Eqs. (19), (21), (23), and (31), respectively, and do not add the EPV bubble diagrams B_1 to B_4 [Eqs. (33), (35), (38), and (40)]. Below we will present numbers

illustrating the importance of these terms. These numbers are obtained by the use of bare interactions. Use of dressed interactions will change the magnitudes of the different terms, but does not resolve the choice between methods with or without inclusion of $B_1 \dots B_4$.

IV. COMPUTATIONAL DETAILS

In this section we present the details of the calculations on Ar, NH_3 , and H_2O . With the methods described above, the multipole moments and polarizabilities of ammonia and water are computed through second order in the correlation. Using the moments and polarizabilities, we calculate the induction and dispersion coefficients by means of equations presented earlier.^{23,25} The Casimir–Polder integral, appearing in these equations, is computed by a ten-point Gauss–Chebyshev quadrature, so that every polarizability must be computed for ten different ω values. We routinely compute also the static polarizabilities.

A. Basis sets and geometries

For the integral evaluation, SCF, and four-index transformation the ATMOL²⁶ suite of programs was used. All calculations are based on spherical Gauss-type orbitals (GTO's).

The Ar basis set was used earlier in a TDCHF study of the potential energy surface of the Ar– H_2O complex.²⁷ It is a (13s 10p 5d 3f 3g/9s 7p 5d 3f 3g) basis of dimension 103.

For the H_2O calculations we used 157 basis functions:²⁸ a primitive (14s 9p 4d 3f 1g) basis contracted to [10s 7p 4d 3f 1g] on oxygen, and a (9s 3p 3d 1f/7s 3p 3d 1f) basis on hydrogen. The oxygen (13s,8p) basis set of Van Duijneveldt²⁹ was extended with a diffuse s ($\alpha_s = 0.07419$) and p orbital ($\alpha_p = 0.0492$); all GTO exponents in this paper are in bohr⁻². The six most compact s orbitals were contracted in a [4,2] contraction and the four most compact p orbitals in a [2,2] contraction. The four d functions have exponents 4.0, 1.218 87, 0.361 02, 0.10, the three f functions have 1.0, 0.3, 0.1, and $\alpha_g = 0.16$. The hydrogen basis set is derived from an 8s set,²⁹ with the four

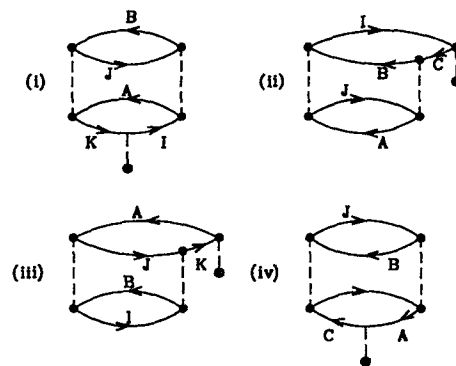


FIG. 3. Brandow diagrams representing the second order correlation contributions to the multipole moment. Also the mirror images of terms (ii) and (iii) must be included. The diagrams correspond to the four respective terms of Eq. (50).

most compact orbitals contracted in a [2,2] contraction. A diffuse s orbital with exponent 0.0292 was added. The p orbitals have exponents 1.5, 0.4, 0.1, and the d exponents are 1.2, 0.3, 0.075. The f orbital has exponent 0.1.

The OH distance is $1.8088 a_0$ and the HOH angle is 104.52° , as in an earlier study on the Ar-H₂O complex.²⁷ The origin was kept on the center of mass with the oxygen atom on the positive z axis and the protons in the xz plane, in accordance with the geometry used in Ref. 27.

For NH₃ the bases N(12s 8p 3d 1f/10s 7p 3d 1f) and H(7s 2p 1d/6s 2p 1d) were used. The resulting 104-dimensional ammonia basis is a more loosely contracted version³⁰ of basis A of Diercksen and Sadlej³¹ with $\alpha_f = 0.25$. This basis set supports an accurate calculation of C_6 and to some extent of C_8 , but not of the higher van der Waals coefficients, since g orbitals on N and f orbitals on H are lacking.

The center of mass was kept at the origin with the N atom lying on the positive z axis and one of the protons in the xz plane. The NH bond makes an angle 112.5° with the threefold symmetry axis, which corresponds to an HNH angle of 106.27° . The experimental³² angle is 106.67° . The NH bond distance is $1.9132 a_0$.

B. Computational requirements

All calculations were performed on an IBM RS/6000 Model 320 workstation with 32MB main memory. The CPU times quoted below refer to this machine. The timings will show that the evaluation of the correlation contribution to the polarizability using the MBPT method can be done with large basis sets on this modest computer.

We have put no restrictions on the correlating orbitals; all orbitals, including those in the core, are included. Point group symmetry is used: only symmetry unique components of the polarizabilities are computed.

The correlation contribution to the permanent moments of water are evaluated in about three minutes of CPU time with the help of Eqs. (51) and (52).

The major part of the CPU time necessary to evaluate the correlation contribution to the polarizability is spent on the contributions A_1 and A_4 . This is because A_1 is evaluated by an n^6 process, and indeed about 90% of the time spent on A_1 is in the evaluation of the matrix elements of F in Eq. (18). The contributions to A_4 are obtained by contracting the wave functions of Eqs. (20)–(29), see Eq. (31). Although the evaluation of these wave functions is an n^5 process, the wave functions depend on the (l,m) quantum numbers of the multipoles and also on the frequency ω , so that a large number of them have to be calculated.

For argon the total computer resources needed are about 40 CPU min and 15MB of memory space. The water calculation required 9 CPU h and 10MB of memory space. The argon atom, with its 18 electrons, requires more memory than water with its 10 electrons, as the required array size scales with the number of occupied and virtual orbitals squared.

TABLE I. Argon properties. All values in a.u. See the text for the definition of the correlation methods A and $A+B$.

	SCF	Energy		Literature	
		MP2	Static polarizabilities		
			A	$A+B$	
	-526.807 189	-0.414 391			-526.8175, ^a -0.706 ^b
	TDCHF				
α_{00}^{11}	10.736	11.120	11.369		11.17, ^c 11.08 ^d
α_{00}^{22}	50.973	53.160	53.366		
α_{00}^{33}	548.88	568.53	570.49		
		Argon-argon dispersion coefficients			
C_6	61.947	65.334	68.456		64.30, ^e 64.20 ^f
C_8	1 564.5	1 666.0	1 711.7		
C_{10}	48 506.0	51 697.0	52 699.0		

^aReference 33, numerical SCF.

^bReference 34, estimate of the MP2 limit in the correlation energy.

^cReference 35, CCSD (T) value corrected for core correlation.

^dReference 36, value from dipole oscillator strength distribution.

^eReference 47, value from dipole oscillator strength distribution.

^fReference 48, value from dipole oscillator strength distribution.

V. RESULTS AND DISCUSSION

In Sec. II we defined the following contributions to the polarizability: A_i , $i=1,\dots,4$, [Eqs. (19), (21), (23), and (31)] and B_i , $i=1,\dots,4$ [Eqs. (33), (35), (38), and (40)]. In the present section method A will refer to $\sum_{i=1}^4 A_i$ and hence this method does not include corrections for the bubble EPV diagrams B_i . Method $A+B$ refers to $\sum_{i=1}^4 (A_i + B_i)$.

The energies and first and second order properties for the three systems argon, water, and ammonia are given and compared to literature values in Tables I to III.

A. Argon

Argon results are presented in Table I. Our SCF energy is $c.$ 0.01 a.u. higher than the Hartree-Fock limit calculated by Froese-Fischer.³³ We recover about 60% of the limit of the MP2 energy estimated by Termath, Klopper, and Kutzelnigg.³⁴ Note here that our basis is primarily meant to describe the polarization of argon; a much larger basis would be needed to describe reliably the ground state correlation energy as well.

Although the differences are not large between method A and method B , the static dipole-dipole polarizability obtained by method A agrees best with accurate literature values. The computed dipole polarizability is close to the CCSD(T) value of Rice *et al.*³⁵ (which includes an estimated correction for the core correlation effect) and to the half-empirical value of Kumar and Meath.³⁶

B. H₂O

The results for the H₂O molecule are presented in Table II. A list of multipole moments and polarizabilities together with references to experimental data can be found in Bulski *et al.*²⁷ and Maroulis.³⁷ Our SCF and MP2 energies are of a good quality: the SCF energy is close to the SCF limit estimate (see, e.g., Ref. 38) and the MP2 energy is about 90% of the estimated MP2 energy limit.³⁸

TABLE II. Properties (in a.u.) of H₂O. See Eq. (50) for definition of the MP2 moments and the text for the definition of correlation methods *A* and *A+B*.

		Energy			
		SCF	MP2	Literature	
		-76.066 810	-0.320 580	-76.0658, ^a -0.3605 ^b	
		Multipole moments			
<i>L</i>	<i>M</i>	SCF	MP2	Total	Literature
1	0	-0.7792	0.051 46	-0.7277	0.7268 ± 0.0004 ^c
2	0	-0.1038	0.000 05	-0.1037	0.10 ± 0.02 ^d
3	0	1.9379	0.363 65	2.3016	
2	2	2.1333	-0.232 48	1.9008	2.205 ± 0.02 ^d
3	2	-3.5833	-0.357 04	-3.9403	
		Static polarizabilities			
		TDCHF	<i>A</i>	<i>A+B</i>	Literature
α_{00}^{11}		8.510	9.470	9.624	9.64, ^c 9.75, ^f 9.77 ^g
α_{11}^{11}		9.174	9.988	10.108	9.81, ^c 10.00, ^f 10.02 ^g
α_{-1-1}^{11}		7.891	8.910	8.961	9.59, ^c 9.56, ^f 9.64 ^g
$\bar{\alpha}$		8.525	9.456	9.565	9.68, ^c 9.77, ^f 9.81 ^g 9.64 ± 0.14 ^h
α_{00}^{21}		-1.959	-2.598	-2.633	-2.194 ⁱ
α_{20}^{21}		-2.717	-2.737	-2.853	-3.433 ^j
α_{11}^{21}		-7.143	-7.760	-7.843	-7.785 ^j
α_{-1-1}^{21}		-1.822	-2.498	-2.509	-2.062 ^j
α_{32}^{22}		40.732	45.407	45.947	
α_{20}^{22}		1.228	1.707	1.843	
α_{11}^{22}		46.425	51.254	51.375	
α_{00}^{22}		37.149	42.018	42.368	
α_{-1-1}^{22}		38.043	43.356	43.398	
α_{-2-2}^{22}		37.604	42.777	42.809	

^aReference 38: SCF value.^bRef. 38: Explicitly correlated MP2 energy.^cReference 40: Experimental value. Conversion factor: 1 D=0.394 487 a.u.^dReference 41: Experimental value.^eReference 43: Calculated with CEPA.^fReference 37: MP2 values.^gReference 49: MP2 values.^hEstimate of Ref. 37.ⁱReference 50: Value from dipole oscillator strength distribution.^jReference 42: CI value.

The dipole moment 0.7277 a.u. is in good agreement with the value 0.725 ± 0.005 estimated by Maroulis³⁷ and in very good agreement with the experimental value of 0.7268 a.u. due to Clough *et al.*⁴⁰ The quadrupole moment Q_0^2 is close to the old value measured by Verhoeven and Dymanus.⁴¹ The correlation correction to Q_0^2 is surprisingly small. The computed Q_2^2 value falls outside the experimental error bars,⁴¹ so that the reliability of this number is open to discussion. Note in this respect that the SCF value is closer to experiment than the MP2 value.

An extensive review of the literature values of the static dipole polarizabilities is given by Maroulis.³⁷ We list here only part of these values. Our TDCHF results are close to the finite-field SCF values that Maroulis obtained with his largest basis set *W*5. The SDQ-MP4 value obtained by Maroulis for $\alpha_{-1,-1}^{1,1}$ is not particularly close to

TABLE III. Properties (in a.u.) of NH₃. See Eq. (50) for definition of the MP2 moments and the text for the definition of correlation methods *A* and *A+B*.

		Energy			
		SCF	MP2	Literature	
		-56.219 851 0	-0.260 541 3	-56.222 85, ^a -0.320 65 ^b	
		Multipole moments			
<i>L</i>	<i>M</i>	SCF	MP2	Total	Literature
1	0	-0.644 52	0.033 96	-0.610 56	-0.5995, ^c -0.5898 ^d -0.5789 ^c
2	0	-2.118 91	-0.040 88	-2.159 79	-2.250, ^c -2.210 ^d
3	0	2.504 99	0.017 63	2.522 62	
3	3	4.259 62	-0.084 82	4.174 80	
		Static polarizabilities			
		TDCHF	<i>A</i>	<i>A+B</i>	Literature
α_{00}^{11}		13.277	14.668	14.841	15.66 ^d
α_{11}^{11}		12.769	13.591	13.784	13.73 ^d
$\bar{\alpha}$		12.938	13.950	14.136	14.37 ^d
$\Delta\alpha^f$		0.508	1.077	1.057	1.93 ^d
α_{00}^{21}		0.413	-0.492	-0.441	
α_{11}^{21}		-5.345	-5.705	-5.783	
α_{20}^{22}		75.629	83.236	84.072	77.01, ^g 90.48 ^d
α_{22}^{22}		70.967	76.207	76.493	71.52, ^g 78.96 ^d
α_{11}^{22}		79.916	88.105	88.259	80.84, ^g 95.88 ^d
α_{21}^{22}		-7.068	-7.118	-5.783	

^aSCF result from Klopper *et al.*, Ref. 38.^bMP2-R12/*A* result from Klopper *et al.*, Ref. 38.^cMP2 result from Diercksen and Sadlej, Ref. 31.^dMP4 value from Diercksen and Sadlej, Ref. 31.^eReference 39, experimental value.^fDefinitions used are $\bar{\alpha} = \frac{1}{3}(\alpha_{00}^{11} + 2\alpha_{11}^{11})$ and $\Delta\alpha = \alpha_{00}^{11} - \alpha_{11}^{11}$.^gSCF value from Diercksen and Sadlej, Ref. 31.

either of our numbers, with both our methods yielding a value that seems to be on the low side. This has the consequence that our isotropic values are also somewhat too low. Since method *A+B* generally seems to overshoot, its average value falls now within the conservatively estimated error bars for the averaged dipole polarizability,³⁷ whereas method *A* gives the corresponding number just outside these error bars. Maroulis' SDQ-MP4 anisotropy seems to be better reproduced by the values of method *A*, although all the values are too low. In any case, addition of second order correlation to TDCHF gives a large improvement for the static polarizabilities with the remaining errors being at most 3%.

The dipole-quadrupole polarizabilities for H₂O are compared in Table II to earlier values of John *et al.*,⁴² who used a smaller basis and the single-double CI method. We also present values for the quadrupole polarizabilities of H₂O in this table.

C. NH₃

We consider the SCF and MP2 energy in Table III. Our SCF energy is in reasonable agreement with the best value of Klopper and Kutzelnigg,³⁸ and our MP2 approach recovers about 80% of the MP2 energy limit.³⁸

In the calculations we have used a more loosely contracted and spherical version of the basis set *A* of Diercksen and Sadlej³¹ (DS). Also our ammonia geometry differs

slightly from theirs (the HNH angles differ by 0.40°). These facts explain that our SCF dipole is 0.0075 a.u. lower than the corresponding value of DS. This also means that the origin of the difference between the respective MP2 values for the dipole lies primarily in the SCF number. A further small discrepancy is caused by the fact that we have used the second order formula (50), whereas DS differentiate twice the MP2 energy computed with finite field orbitals. Since DS show that the MP2 method yields the main part of the correlation correction to the dipole moment, the present MP2 dipole can be expected to be an accurate number.

Our SCF and MP2 quadrupole are, respectively, 0.033 and 0.090 a.u. higher than the corresponding ones of DS. The small disagreement between the MP2 corrections must be attributed either to the use of finite field orbitals by DS or to the greater flexibility in our basis. The analysis of DS indicates that third and fourth order correlation raises the quadrupole by 0.040 a.u., so that our MP2 value differs somewhat fortuitously only by 0.0050 a.u. from the MP4 value of DS. As remarked by DS, their basis set is not flexible enough to provide reliable estimates of the octupole and higher properties. Since we have used essentially the same basis, the same remark applies also to our results.

We can also compare static polarizabilities with the work of DS. Their and our SCF values of α_{00}^{11} differ by 0.05 a.u. and the SCF α_{11}^{11} values agree within rounding errors. For α_{00}^{11} DS found at the MP2 level a value of 15.73 a.u.; their full MP4 value is 15.66 a.u. We find 14.67 a.u. in method *A* and 14.84 a.u. in method *A+B*. So, our result disagrees with the DS value. Moreover, contrary to our experience so far, method *A+B* seems to perform better. The correlated values for α_{11}^{11} show better agreement. Method *A*: 13.59, method *A+B*: 13.78, MP2: 13.74, MP4: 13.73, all values in a.u. In order to see if we could explain the relatively large difference in the MP2 values of α_{00}^{11} we computed the correlated dipole moment by means of finite-field orbitals and differentiated this moment with respect to the field. It can be shown that this procedure gives diagrammatically the dressing of one of the external field vertices by an infinite series of bubbles. Our results from this calculation are $\alpha_{00}^{11}=14.82$ and $\alpha_{11}^{11}=13.52$ a.u., and we see that the operator dressing cannot explain the fairly large disagreement between the DS value of α_{00}^{11} and ours. The differentiation of the moment gives a few terms that the differentiation of the energy does not give. This fact or the differences in the basis must be responsible for the disagreement.

In Table III we also present quadrupole–quadrupole polarizabilities and compare these with the corresponding numbers of DS. In order to facilitate comparison with the DS numbers, which are given in the Buckingham⁴⁴ convention, we present the following formulas which are derived under the assumption of C_{3v} symmetry. The negative *m* values refer to sine-type harmonics and the positive values to cosine types,

$$\begin{aligned}\alpha_{0,0}^{2,2} &= 3C_{zz,zz}, \\ \alpha_{-2,-2}^{2,2} &= \alpha_{2,2}^{2,2} = 4C_{xy,xy} = 4(C_{xx,xx} - \frac{1}{4}C_{zz,zz}), \\ \alpha_{-1,-1}^{2,2} &= \alpha_{1,1}^{2,2} = 4C_{xz,xz}, \\ -\alpha_{-2,-1}^{2,2} &= \alpha_{2,1}^{2,2} = 4C_{xx,xz} = -4C_{yy,xz}.\end{aligned}\quad (55)$$

Note that DS present values for $C_{xy,xy}$ which are redundant, but do not give $C_{xx,xz}$ values, so that we can compare only three out of the four linear independent components. Again we find a larger disagreement with the work of DS than might be expected from the close similarity of bases and methods. It is quite conceivable that we find here yet another illustration of the sensitivity of polarizabilities for AO basis sets.

D. van der Waals coefficients

General expressions for the van der Waals coefficients are given by Van der Avoird, Wormer, Mulder, and Berns²⁵ and in Ref. 45. We will present induction and dispersion coefficients for the complexes Ar–Ar, H₂O–H₂O, and Ar–NH₃ that are computed as described in these references. The coefficients are for use in the following expression for the long range energy:

$$\begin{aligned}\Delta E &= \sum_{n=6}^{10} \frac{1}{R^n} \sum_{\substack{L_A, K_A \\ L_B, K_B, L}} C_n^{L_A K_A L_B K_B L} \\ &\times \sum_{M_A, M_B, M} \begin{pmatrix} L_A & L_B & L \\ M_A & M_B & M \end{pmatrix} \\ &\times D_{M_A K_A}^{L_A}(\omega_A) * D_{M_B K_B}^{L_B}(\omega_B) * C_M^L(\Omega),\end{aligned}\quad (56)$$

where the quantity between large brackets is a Wigner $3j$ -symbol, ω_A and ω_B are the Euler angles of monomers *A* and *B*, $D_{M,K}^L(\omega)$ is a Wigner *D* matrix in the convention of Ref. 46 and $C_M^L(\Omega)$ is a spherical harmonic function normalized to $4\pi/2L+1$. The quantity Ω refers to the polar angles of the vector **R** that points from the mass center of *A* to the mass center of *B*. *R* is its length. Note that the angular function can be reduced considerably if one of the monomers, say *A*, is an atom. Since then $L_A=K_A=0$, the $3j$ -symbol shrinks to a phase times $1/\sqrt{2L+1}$. This factor may be incorporated into the definition of the van der Waals coefficient, cf. Ref. 27.

Both methods, *A* and *B*, overcorrect a little the TD-CHF value for the C_6 coefficient of Ar–Ar, which lies below the most reliable literature values,^{47,48} see Table I. Again method *A* is more accurate and overshoots by only 1.5%. Since the higher polarization function space is less saturated than the *s p d* space, the errors in C_8 and C_{10} are probably larger, but, nevertheless, we believe our values obtained by method *A* to be the most accurate ones published to date.

We expect our basis set for H₂O to support rather reliable calculations of the van der Waals coefficients for the water dimer up to and including C_{10} . This is confirmed by the isotropic C_6 obtained by method *A*, which is only

TABLE IV. Correlation effects on the most important van der Waals coefficients for the H₂O–H₂O complex.

L_A	K_A	L_B	K_B	L	n	TDCHF	A	$A+B$	Literature ^a
0	0	0	0	0	6	39.437	46.443	47.623	48.794
2	2	0	0	2	6	3.065	3.003	3.207	3.178
1	0	0	0	1	7	79.552	102.16	104.58	170.01
3	2	0	0	3	7	33.841	36.55	38.11	40.32
0	0	0	0	0	8	947.39	1 141.7	1 161.6	1 227.5
2	2	0	0	2	8	162.27	134.6	141.9	170.5
1	0	0	0	1	9	2 514.9	3 275.3	3 335.4	5 357.2
3	2	0	0	3	9	2 394.6	2 742.0	2 809.5	3 062.4
0	0	0	0	0	10	26 507.0	33 441.0	33 855.0	32 357.0
1	0	1	0	2	10	-5 162.0	-7 236.0	-7 376.0	-17 818.0

^aReference 45, method $A+B$ in a 91-dimensional basis.

2.3% higher than the accurate value 45.37 a.u. of Zeiss and Meath.⁵⁰ They obtained this number from an empirical dipole oscillator strength distribution. In Table IV we illustrate the importance of correlation and basis set for dispersion coefficients. A true correlation effect of as much as

20% is found in the first C_7 . Note also that this coefficient is extremely basis dependent: by going from a 91-dimensional water basis to the present 157-dimensional one, it drops from 170.01 to 104.58 a.u. (in method $A+B$)! We wish to reiterate that this is *not* an artifact of the mul-

TABLE V. Selected dispersion coefficients (a.u.) of H₂O–H₂O computed by method A . A coefficient $C_n^{L_A K_A L_B K_B L}$, $x\%$ smaller in absolute value than the largest with the same n is discarded, where $x=1$ for C_6 and C_7 ; $x=5$ for C_8 and C_9 ; and $x=10$ for C_{10} .

L_A	K_A	L_B	K_B	L	n	L_A	K_A	L_B	K_B	L	n		
0	0	0	0	0	6	46.443	3	-2	0	0	3	9	2 742.0
2	-2	0	0	2	6	3.003	3	0	0	0	3	9	-1 976.4
2	2	0	0	2	6	3.003	3	2	0	0	3	9	2 742.0
2	-2	2	-2	4	6	0.52	3	-2	2	-2	5	9	188.9
2	2	2	-2	4	6	0.52	3	-2	2	2	5	9	188.8
2	2	2	2	4	6	0.52	3	2	2	-2	5	9	188.8
1	0	0	0	1	7	102.16	3	2	2	2	5	9	188.9
2	-2	1	0	3	7	-4.70	4	-2	1	0	5	9	-216.2
2	2	1	0	3	7	-4.70	4	0	1	0	5	9	244.3
3	-2	0	0	3	7	36.55	4	2	1	0	5	9	-216.2
3	0	0	0	3	7	-28.39	4	-4	3	-2	7	9	-184.0
3	2	0	0	3	7	36.55	4	-4	3	2	7	9	-184.0
3	-2	2	-2	5	7	6.96	4	-2	3	-2	7	9	-403.0
3	-2	2	2	5	7	6.96	4	-2	3	0	7	9	313.2
3	0	2	-2	5	7	-5.40	4	-2	3	2	7	9	-403.0
3	0	2	2	5	7	-5.40	4	0	3	-2	7	9	454.7
3	2	2	-2	5	7	6.96	4	0	3	0	7	9	-353.4
3	2	2	2	5	7	6.96	4	0	3	2	7	9	454.7
0	0	0	0	0	8	1141.7	4	2	3	-2	7	9	-403.0
1	0	1	0	2	8	-186.8	4	2	3	0	7	9	313.2
2	-2	0	0	2	8	134.6	4	2	3	2	7	9	-403.0
2	0	0	0	2	8	71.5	4	4	3	-2	7	9	-184.0
2	2	0	0	2	8	134.6	4	4	3	2	7	9	-184.0
3	-2	1	0	4	8	-68.8	5	-4	0	0	5	9	299.7
3	2	1	0	4	8	-68.8	5	4	0	0	5	9	299.7
3	-2	3	-2	6	8	-116.3	0	0	0	0	0	10	33 441.0
3	0	3	-2	6	8	90.3	1	0	1	0	2	10	-7 236.0
3	0	3	0	6	8	-70.2	3	-2	1	0	4	10	-5 980.0
3	2	3	-2	6	8	-116.3	3	0	1	0	4	10	4 308.0
3	2	3	0	6	8	90.3	3	2	1	0	4	10	-5 980.0
3	2	3	2	6	8	-116.3	3	-2	3	-2	6	10	-4 308.0
4	-2	0	0	4	8	98.7	3	2	3	-2	6	10	-4 301.0
4	0	0	0	4	8	-111.5	3	2	3	2	6	10	-4 308.0
4	2	0	0	4	8	98.7	4	-2	0	0	4	10	6 413.0
1	0	0	0	1	9	3275.3	4	0	0	0	4	10	-7 048.0
2	-2	1	0	3	9	-240.8	4	2	0	0	4	10	6 413.0
2	2	1	0	3	9	-240.8							

TABLE VI. Selected induction coefficients (a.u.) of H₂O–H₂O computed with MP2 moments and static polarizabilities from method *A*. A coefficient $C_n^{L_A K_A L_B K_B L}$ $x\%$ smaller in absolute value than the largest with the same n is discarded, where $x=1$ for C_6 and C_7 and $x=5$ for C_8 .

L_A	K_A	L_B	K_B	L	n		L_A	K_A	L_B	K_B	L	n	
0	0	0	0	0	6	5.0076	3	-2	1	0	4	8	-91.12
2	0	0	0	2	6	11.1974	3	2	1	0	4	8	-91.12
2	0	2	-2	2	6	0.1393	3	-2	3	-2	6	8	-157.49
2	0	2	-2	4	6	1.5044	3	0	3	-2	6	8	16.31
1	0	0	0	1	7	-4.451	3	0	3	0	6	8	-12.86
2	0	1	0	1	7	3.997	3	2	3	-2	6	8	-157.49
2	0	1	0	3	7	-19.938	3	2	3	0	6	8	124.20
3	-2	0	0	3	7	43.774	3	2	3	2	6	8	-157.49
3	0	0	0	3	7	-4.532	4	-4	0	0	4	8	91.88
3	2	0	0	3	7	43.774	4	-2	0	0	4	8	135.76
3	-2	2	-2	5	7	6.610	4	0	0	0	4	8	-113.40
3	-2	2	2	5	7	6.610	4	2	0	0	4	8	135.76
3	0	2	-2	5	7	-0.684	4	4	0	0	4	8	91.88
3	0	2	2	5	7	-0.684	4	-4	2	-2	6	8	17.33
3	2	2	-2	5	7	6.61	4	-4	2	2	6	8	17.33
3	2	2	2	5	7	6.61	4	-2	2	-2	6	8	21.31
0	0	0	0	0	8	110.93	4	-2	2	2	6	8	21.31
2	-2	0	0	2	8	174.45	4	0	2	-2	6	8	-17.29
2	0	0	0	2	8	-206.22	4	0	2	2	6	8	-17.29
2	2	0	0	2	8	174.45	4	2	2	-2	6	8	21.31
2	0	2	0	4	8	12.86	4	2	2	2	6	8	21.31
3	-2	1	0	2	8	17.65	4	4	2	-2	6	8	17.33
3	2	1	0	2	8	17.65	4	4	2	2	6	8	17.33

tipole expansion, supermolecule calculations will show the same sensitivity in the long range.

In order to keep the number of H₂O–H₂O coefficients within reasonable limits, Tables V and VI are reduced by deleting all coefficients that are smaller than the largest value of the same n by a certain percentage and furthermore by using the symmetry relationship

$$C_n^{L_A K_A L_B K_B L} = (-)^n C_n^{L_B K_B L_A K_A L} = (-)^L C_n^{L_B K_B L_A K_A L}. \quad (57)$$

An additional requirement, following from the symmetry of the water molecule, is that K_A and K_B must be even in order to obtain a nonvanishing coefficient. Since the leading dispersion coefficients are an order of magnitude larger than the corresponding induction coefficients, Table VI contains only induction coefficients through $n=8$. Note, however, that the anisotropic induction coefficients are not

TABLE VII. van der Waals coefficients (a.u.) for the complex Ar–NH₃ with Ar as monomer A.

L_B	K_B	n	TDCHF	<i>A</i>	<i>A+B</i>
0	0	6	69.170	75.216	78.143
2	0	6	-1.864	-0.359	-0.484
1	0	7	-88.926	-105.70	-108.98
3	-3	7	76.215	78.78	82.68
3	0	7	62.579	59.95	63.35
3	3	7	-76.215	-78.78	-82.68
0	0	8	1917.5	2115.0	2165.3
2	0	8	153.9	342.8	348.5
4	-3	8	-289.4	-303.0	-318.4
4	0	8	-61.3	-79.3	-77.5
4	3	8	289.4	303.0	318.4

smaller than their dispersion counterparts. Finally, we decided, because of space limitations, to present in Table V only dispersion coefficients obtained by method *A*. We believe this to be a theoretically sounder method and also it seems to give somewhat better results than method *A+B*.

For the Ar–NH₃ complex we present the van der Waals coefficients up to and including C_8 in Table VII, the ammonia basis being inadequate for the computation of higher dispersion coefficients. Even for the polarizability α_{mm}^{31} , which contributes to the C_8 coefficients, g orbital(s) are required. However, its components are relatively small and do not affect the accuracy of the C_8 coefficients too much. In Table VIII the corresponding induction coefficients are listed.

VI. SUMMARY AND CONCLUSIONS

We have presented a method for correcting TDCHF frequency-dependent polarizabilities and van der Waals co-

TABLE VIII. Induction coefficients for Ar–NH₃ obtained from (i) the SCF moments combined with TDCHF polarizabilities, (ii) MP2 moments combined with polarizabilities from method *A*, and (iii) MP2 moments with polarizabilities from method *A+B*.

L_B	K_B	n	SCF	<i>A</i>	<i>A+B</i>
0	0	6	4.4597	4.2382	4.1454
2	0	6	9.9723	9.4770	9.2694
1	0	7	-91.421	-93.482	-91.434
3	0	7	-93.099	-95.197	-93.112
0	0	8	125.24	129.28	127.35
2	0	8	80.14	90.89	90.50
4	-3	8	-118.16	-116.18	-113.63
4	0	8	37.35	54.46	53.27
4	3	8	118.16	116.18	113.63

efficients by true second-order correlation. The approach is based on a double perturbation theory with one perturbation being the monochromatic external electric field and the other the Møller–Plesset correlation potential.

The final formulas are given in the form in which they are implemented in our new computer code, which is almost 3 orders of magnitude faster than our earlier code. Calculations are now possible for closed shell molecules in basis sets large enough to give accurate values for the van der Waals coefficients. For instance, for the water molecule a basis (including a *g* orbital) of dimension 157 was used and the complete second order correlation contribution for 66 polarizability components and 11 frequencies was computed on a RS/6000-320 work station in about 9 h of CPU time.

As we noted in Sec. II, a fully consistent MBPT treatment of correlation effects yields a cancellation of all the exclusion principle violating (EPV) terms. The TDCHF method, on the other hand, includes terms that from the point of view of MBPT are EPV, although from the point of view of TDCHF they are not, of course. Since it is thus not *a priori* clear whether these terms must be included, we computed polarizabilities with (method *A+B*) and without (method *A*) the TDCHF EPV terms. On the whole, method *A* seems to give the more reliable results, with both methods giving large improvements to TDCHF. Since in an exact theory all the EPV terms are absent, we believe *A* to be the better method.

We have also given an π^5 expression for multipole moments correct to second order in the correlation. For water and ammonia the moments obtained by this formula are close to the experimental values, and we may conclude that MP2 seems to account for the majority of the correlation effects on the multipoles. From the correlated moments and polarizabilities we obtain rather simply correlated induction coefficients.

In all our calculations we found that large basis sets, including many polarization functions, are required. We believe that further quantitative improvement of our results will be found sooner in the use of larger bases than in better correlation methods.

ACKNOWLEDGMENTS

The authors thank Professor A. van der Avoird for critically reading the manuscript and useful comments. This research has been supported in part by the Netherlands Foundation for Chemical Research (SON) with financial aid from the Netherlands Organization for Scientific Research (NWO). Part of the work has been performed as an IBM Academic Information Systems project.

¹J. Gwo, M. Havenith, K. L. Busarov, R. C. Cohen, C. A. Schuttenmaer, and R. J. Saykally, *Mol. Phys.* **95**, 793 (1991).

²E. Zwart and W. L. Meerts, *Chem. Phys.* **95**, 793 (1991).

³E. Zwart, H. Linnartz, W. L. Meerts, G. T. Fraser, D. D. Nelson, and

W. Klemperer, *J. Chem. Phys.* **95**, 793 (1991).

⁴J. W. I. van Bladel, A. van der Avoird, and P. E. S. Wormer, *J. Phys. Chem.* **95**, 5414 (1991).

⁵H. B. G. Casimir and D. Polder, *Phys. Rev.* **73**, 360 (1948).

⁶F. Visser, P. E. S. Wormer, and P. Stam, *J. Chem. Phys.* **76**, 4973 (1983).

⁷H. Hettema and P. E. S. Wormer, *J. Chem. Phys.* **93**, 3389 (1990).

⁸M. C. van Hemert and C. E. Blom, *Mol. Phys.* **43**, 229 (1981).

⁹J. Olsen and P. Jørgensen, *J. Chem. Phys.* **82**, 3225 (1985).

¹⁰P. Jørgensen, H. J. Aa. Jensen, and J. Olsen, *J. Chem. Phys.* **89**, 3654 (1988).

¹¹J. Olsen, H. J. Aa. Jensen, and P. Jørgensen, *J. Comput. Phys.* **74**, 265 (1988).

¹²H. Hettema, H. J. Aa. Jensen, P. Jørgensen, and J. Olsen, *J. Chem. Phys.* **97**, 1174 (1992).

¹³E. Dalgaard and H. J. Monkhorst, *Phys. Rev. A* **28**, 1217 (1983).

¹⁴H. Koch and P. Jørgensen, *J. Chem. Phys.* **93**, 3333 (1990).

¹⁵P. E. S. Wormer and W. Rijks, *Phys. Rev. A* **33**, 2928 (1986).

¹⁶J. E. Rice and N. C. Handy, *J. Chem. Phys.* **94**, 4959 (1991).

¹⁷A. J. Sadlej, *J. Chem. Phys.* **75**, 320 (1981).

¹⁸S. Rybak, B. Jeziorski, and K. Szalewicz, *J. Chem. Phys.* **95**, 6576 (1991).

¹⁹J. Paldus and J. Čížek, *Adv. Quantum Chem.* **9**, 105 (1975).

²⁰J. Paldus, Lecture notes, Nijmegen (1981) (unpublished).

²¹P. W. Langhoff, S. T. Epstein, and M. Karplus, *Rev. Mod. Phys.* **44**, 602 (1972).

²²W. Rijks, *A Study of the Effects of Intramolecular Correlation on Intermolecular Interactions*, Ph. D. thesis, University of Nijmegen, 1989.

²³W. Rijks and P. E. S. Wormer, *J. Chem. Phys.* **88**, 5704 (1988).

²⁴T. C. Caves and M. Karplus, *J. Chem. Phys.* **50**, 3649 (1969).

²⁵A. van der Avoird, P. E. S. Wormer, F. Mulder, and R. M. Berns, *Top. Current Chem.* **93**, 1 (1980).

²⁶V. R. Saunders and M. F. Guest, Daresbury Laboratory, Warrington, UK, and P. J. Knowles, University of Sussex, UK.

²⁷M. Bulski, P. E. S. Wormer, and A. van der Avoird, *J. Chem. Phys.* **94**, 8096 (1991).

²⁸M. Bulski (private communication).

²⁹F. B. van Duijneveldt, IBM report RJ 945 (1971).

³⁰P. Valiron (private communication).

³¹G. H. F. Diercksen and A. J. Sadlej, *Mol. Phys.* **57**, 509 (1987).

³²Y. Morino, K. Kuchitsu, and S. Yamamoto, *Spectrochim. Acta A* **24**, 335 (1968).

³³C. Froese Fischer, *The Hartree–Fock Method for Atoms* (Wiley, New York, 1977).

³⁴V. Termath, W. Klopper, and W. Kutzelnigg, *J. Chem. Phys.* **94**, 2002 (1991).

³⁵J. E. Rice, P. R. Taylor, T. J. Lee, and J. Almlöf, *J. Chem. Phys.* **94**, 4972 (1991).

³⁶A. Kumar and W. J. Meath, *Can. J. Chem.* **63**, 1616 (1985).

³⁷G. Maroulis, *J. Chem. Phys.* **94**, 1182 (1991).

³⁸W. Klopper and W. Kutzelnigg, *J. Chem. Phys.* **94**, 2020 (1991).

³⁹M. D. Marshall and J. S. Muentzer, *J. Mol. Spectrosc.* **85**, 322 (1982).

⁴⁰S. A. Clough, Y. Beers, G. P. Klein, and L. S. Rothman, *J. Chem. Phys.* **59**, 2254 (1973).

⁴¹J. Verhoeven and A. Dymanus, *J. Chem. Phys.* **52**, 3222 (1970).

⁴²I. G. John, G. B. Bacskay, and N. S. Hush, *Chem. Phys.* **51**, 49 (1980).

⁴³H. J. Werner and W. Meyer, *Mol. Phys.* **31**, 855 (1976).

⁴⁴A. D. Buckingham, in *Intermolecular Interactions—From Diatomics to Biopolymers*, edited by B. Pullman (Wiley, New York, 1978).

⁴⁵W. Rijks and P. E. S. Wormer, *J. Chem. Phys.* **90**, 6507 (1989); **92**, 7454(E) (1990).

⁴⁶D. M. Brink and G. R. Satchler, *Angular Momentum*, 2nd ed. (Oxford University, Oxford, 1968).

⁴⁷A. Kumar and W. J. Meath, *Mol. Phys.* **54**, 823 (1985).

⁴⁸P. J. Leonard and J. A. Barker, in *Theoretical Chemistry, Advances and Perspectives*, edited by H. J. Eyring and D. Henderson, Vol. 1 (Academic, New York, 1975).

⁴⁹G. H. F. Diercksen, V. Kellö, and A. J. Sadlej, *J. Chem. Phys.* **79**, 2918 (1983).

⁵⁰G. D. Zeiss and W. J. Meath, *Mol. Phys.* **33**, 1155 (1977).